

Impact of Birefringence on In-Ice Radio Detectors of Ultra-High Energy Neutrinos

Nils Heyer^{a,*} and Christian Glaser^a

^a*Dept. of Physics and Astronomy, Uppsala University, Box 516, S-75120 Uppsala, Sweden*

E-mail: nils.heyer@physics.uu.se, christian.glaser@physics.uu.se

The planned in-ice radio array of IceCube-Gen2 at the South Pole will provide unprecedented sensitivity to ultra-high-energy (UHE) neutrinos in the EeV range. A good understanding and modeling of the propagation of radio waves through the ice are crucial for the interpretation of experimental data, in particular, for reconstructing the neutrino's energy, direction, and flavor from the detected radio flashes. The birefringent properties of the ice split up the radio pulse into two orthogonal polarization components with slightly different propagation speeds. This provides useful signatures to determine the neutrino energy and is potentially important to determine the neutrino direction to degree precision. Here, we study birefringence in the ice by calculating its effect from first principles. We integrated the calculations into the NuRadioMC simulation code and compared our predictions to in-situ measurements from the ARA and ARIANNA detectors at the South Pole which showed good agreement within the experimental uncertainties. Furthermore, we present the results of a systematic MC study on how birefringence affects the sensitivity of in-ice radio detectors.

38th International Cosmic Ray Conference (ICRC2023)
26 July - 3 August, 2023
Nagoya, Japan



*Speaker

1. Introduction

The IceCube neutrino observatory is the largest neutrino observatory in the world instrumenting a gigatonne of ice with optical modules and has successfully measured the cosmic neutrino flux in the TeV to PeV range [1]. As the flux decreases quickly with energy, a new kind of detector is needed to obtain sensitivity to ultra-high-energy neutrinos in the EeV range. The new detector has to instrument at least a teratonne of ice to be sensitive enough. The radio technique [2], utilizing the Askaryan emission from a neutrino interaction offers the opportunity to do this in a cost-effective way. The first proposed detectors that would be large enough which can expect to measure a neutrino in the EeV range within their lifetime are the Radio-Neutrino-Observatory in Greenland (RNO-G) [3] and the radio component of IceCube-Gen2 [4–6]. As the medium which these detectors are going to use is natural ice and snow, compiled over thousands of years, and not an artificially made detector material with radio detection in mind, the largest systematic uncertainty of future in-ice radio detectors is the ice modeling. Many artifacts within the ice can alter and obstruct the radio pulses that the detectors are hoping to detect and therefore impact their capability to reconstruct the neutrino’s energy, direction, and flavor. These artifacts include temperature and density gradients, ash, dust, and air bubbles trapped in the ice, as well as glacial ice flow which can turn ice into a birefringent medium such as at the South Pole [7].

Birefringence occurs when a crystal has different refractive indices for electromagnetic waves propagating through it at different directions and polarizations. If that happens the wave can split into two distinct polarization eigenstates defined only by the propagation direction, and the dielectric tensor of the ice. The ice at the South Pole was shown to be biaxial birefringent, meaning that electromagnetic waves propagating in all directions through the ice are in some way affected by it [7, 8]. In particular, the propagation velocity and polarization eigenstates of the electric field are subject to changes that can potentially be measured. The IceCube neutrino observatory has successfully parametrized the effect for optical wavelength and incorporated it into the ice model and reconstruction algorithms. This parametrization has resulted in improved in-ice propagation simulations which had a better agreement with pulser measurements [9]. As the wavelengths of radio waves are different from optical waves and the propagation distances of the neutrino-induced pulses are longer due to the different instrumentation techniques, different modeling is needed that characterizes birefringence for in-ice radio detectors. In this contribution, we present a model of birefringence for in-ice radio propagation derived from first principles [10] and study the effects birefringence causes in the detection and reconstruction when including it in the simulations.

2. Birefringence Model

Before studying the effect of birefringence on a radio pulse, the ice model has to be adjusted to describe a birefringent medium. The refractive index at the South Pole changes from ~ 1.35 close to the surface and ~ 1.78 at depths below -200 m. Birefringence, however, has a propagation direction-dependent aspect to it. The direction dependence on the refractive index was measured in [11] and further described in [7]. The new ice model is then a combination of the measured depth and direction-dependent birefringence effect and the previously used depth-dependent model for the index-of-refraction, where we use an exponential parameterization. We note that our code

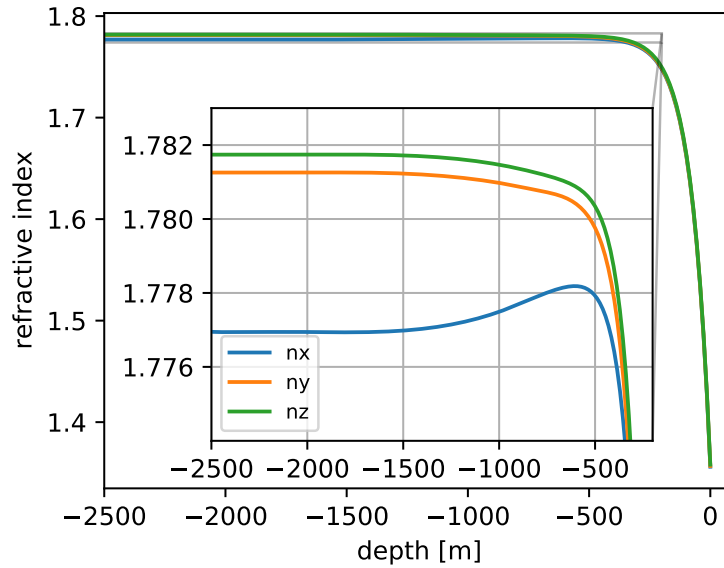


Figure 1: The birefringence ice model showing the refractive index for different directions against depth. The inner plot is a display of the zoomed-in deviations at deep depths. Figure from [10].

is flexible enough to include more accurate descriptions of either in the future. The resulting ice model can be seen in Figure 1, where most depths show a significant but constant difference for the different directions that only converge at shallow depths. Even though the absolute difference in refractive index between directions appears small, it can change radio pulses significantly as they propagate through the ice for more than 1 km due to the long attenuation length [12]. For any radio pulse traveling in any direction, two effective refractive indices can be calculated that define the propagation speed and the polarization of the two eigenstates [10].

Using this ice model, a numerical propagation code was developed that returns the expected electric field at a given antenna position for a given neutrino vertex position and the induced electric field of the neutrino interaction. The propagation code takes the induced electric field and, for every incremental step of the propagation, rotates the pulse from its natural basis (Θ , Φ) into the birefringence eigenbasis (N_1 , N_2) defined by the effective refractive indices and the corresponding polarization eigenvectors, applies a time shift according to the numerical step size and rotates the pulse back into the natural basis (Θ , Φ). This way the interference between the two birefringence eigenstates can be taken into account. An example of a single propagation step can be seen in Figure 2. The result is an electric field modified by the effects it experienced due to birefringence as it would arrive at a given antenna location. It can then be folded with the antenna response to calculate the voltage trace measured by the antenna. The propagation code was integrated into and is publicly available through the Monte Carlo framework NuRadioMC [13].

3. Comparison to Measurements

Although it is difficult to measure and deduce the effects of birefringence from a measurement of radio pulses certain methods exist which allow for such a comparison. The SPIce borehole

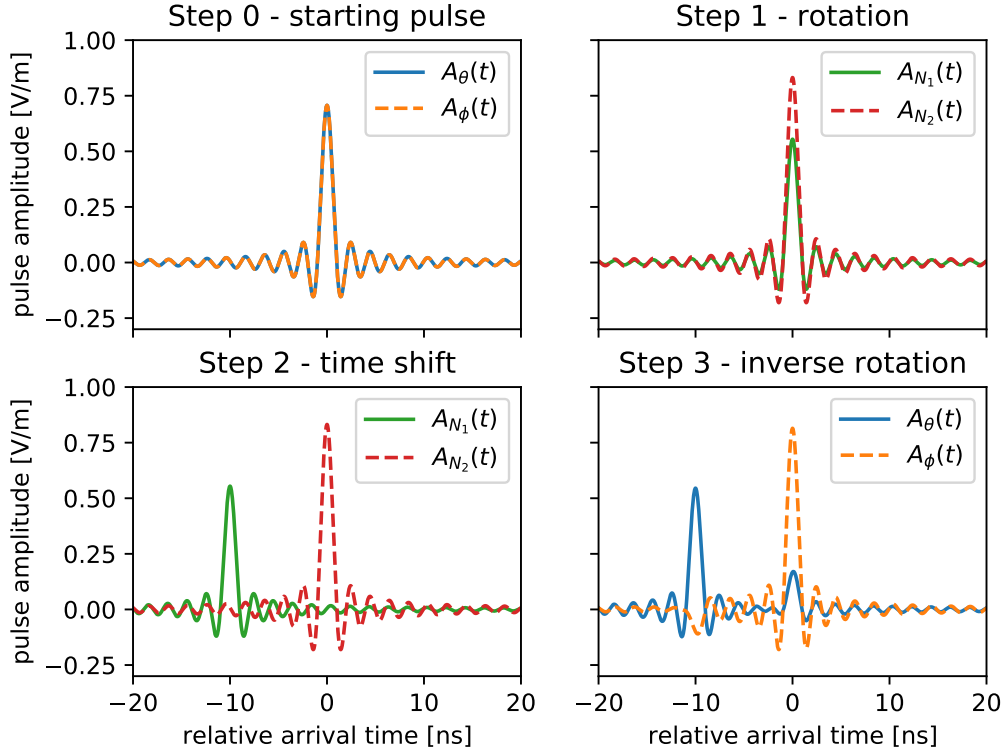


Figure 2: One incremental step in the numerical pulse propagation including the initial waveforms of the theta and phi components (step 0), the rotation into the basis of the birefringence eigenstates (step 1), applying a time shift to separate the pulses (step 2), and the inverse rotation back into the natural basis. Figure from [10].

[14] at the South Pole can be used to lower a radio emitter down to a depth of several kilometers. The radio pulses measured at the surface can be compared to the simulations given the emitter and antenna position and the emitted electric field. The ARA [15] collaboration has published time delays between the antennas sensitive to the vertical polarization component (Vpol) and the antennas sensitive to the horizontal polarization component (Hpol) components of such a measurement. The time delay measured when propagating radio pulses from the emitter in the borehole at a depth of -1000 m to the ARA A2 station was (-14.1 ± 2.8) ns [7]. The simulation for the same geometry showed a time delay of (-10.9 ± 0.4) ns [10]. The time delay measured when propagating radio pulses from the emitter in the borehole at a depth of -1000 m to the ARA A4 station was (4.6 ± 9.0) ns [7]. The simulation for the same geometry showed a time delay of (3.9 ± 0.2) ns [10]. Our modeling improved the agreement with data significantly compared to previous simplified models. Both geometries showed good agreement between simulations and measurements. Furthermore, the ARIANNA [16] collaboration has published the measured polarization depending on the depth of the radio emitter [17] which fluctuated around the naive expectation by a few degrees. It was speculated, that the cause of the fluctuations was birefringence [8], however, our detailed simulation including birefringence found that birefringence does not result

in a significant change in polarization for the geometry probed by the ARIANNA measurement [10]. More measurements of polarization changes and time delays are needed to make further comparisons between simulations and measured data possible. An additional test of the simulations planned for the future is to compare the presented propagation code to highly accurate but very computationally expensive FDTD simulations [18]. However, these simulations also rely on the correct parametrization of the ice model.

4. Impact on the Neutrino detectors

The first step in analyzing the impact of birefringence on in-ice neutrino detectors is to quantify the effect it has on the sensitivity of the experiments, more explicitly, the effective volume. Since birefringence modulates the amplitudes of the propagating electric field the possibility exists that certain trigger criteria are not met anymore when taking birefringence into account or that certain trigger criteria are only met when taking birefringence into account. To investigate these claims, in-ice simulations were performed using the implementation of the propagation code in NuRadioMC [13]. The simulations used a simplified version of a radio detector station planned to be built by the IceCube Gen2 collaboration. We approximate the *deep* trigger by a single Vpol antenna at a depth of -150 m and the *shallow* trigger by two Log-Periodic-Dipole-Array (LPDA) antennas oriented perpendicular to each other at a depth of -3 m where we require a noiseless high-low trigger for any of the three antennas. Usually, the trigger conditions require a coincidence trigger for the shallow LPDA antennas and a power-integrated trigger from the deep Vpol antennas. However, as we want to characterize the systematic effect of birefringence, we trigger on the noiseless waveforms where a single high-low trigger is equivalent to the triggers usually used on noisy waveforms. In order to reduce the showers that had to be simulated with the computationally expensive birefringence propagation, a pre-trigger simulation was run with a $0.1 \times V_{RMS}$ -noiseless-trigger simulated without birefringence. The events which were recorded by the pre-trigger were then simulated with and without birefringence for a trigger threshold of $2 \times V_{RMS}$. Higher trigger thresholds were also investigated but did not show a significant difference from the $2 \times V_{RMS}$ -trigger. After the simulation, the fraction of the effective volume in an isotropic medium was compared to the effective volume in a birefringent medium. For the Vpol, only the triggers on the single Vpol were considered and for the LPDA's one out of two of the antennas had to trigger in order to be counted towards the effective volume. The errors on the fraction were calculated using bootstrapping. We present the results in Figure 3. The larger error margins on the LPDA trigger stem from the lower statistics in our data set as the effective volume of a single detector station is smaller closer to the surface.

When comparing the events that were only triggered when using an isotropic medium or a birefringent medium, the LPDA trigger gained about 20% of events while losing about 10% and the Vpol trigger gained about 5% of events while losing about 10%. In Figure 3 the energy dependence of the relative change in effective volume between the isotropic and the birefringent case is displayed. It shows that a detector solely relying on a Vpol trigger would lose more events (up to 5%) in a birefringent medium than it would gain while the LPDA trigger would gain up to about 10% of events compared to the events it loses. The two antenna types behave differently. This comes from the fact that birefringence does not change the overall fluence of the electric field, it only shifts it from one polarization component to the other. The strength of the effect also depends

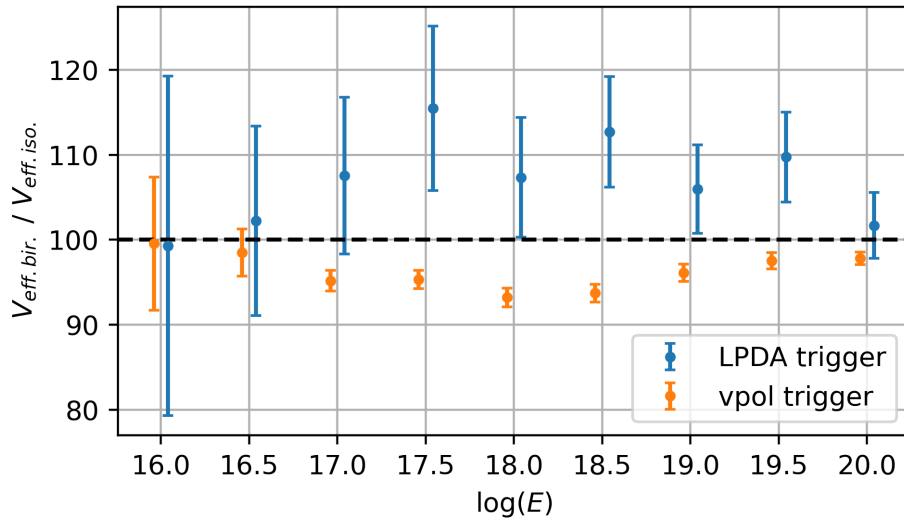


Figure 3: Percent fraction of the effective volume in a birefringent medium and the effective volume in an isotropic medium against neutrino energy. The points were shifted slightly off their true neutrino energy to display the error bars of the LPDA and the Vpol trigger in the same plot.

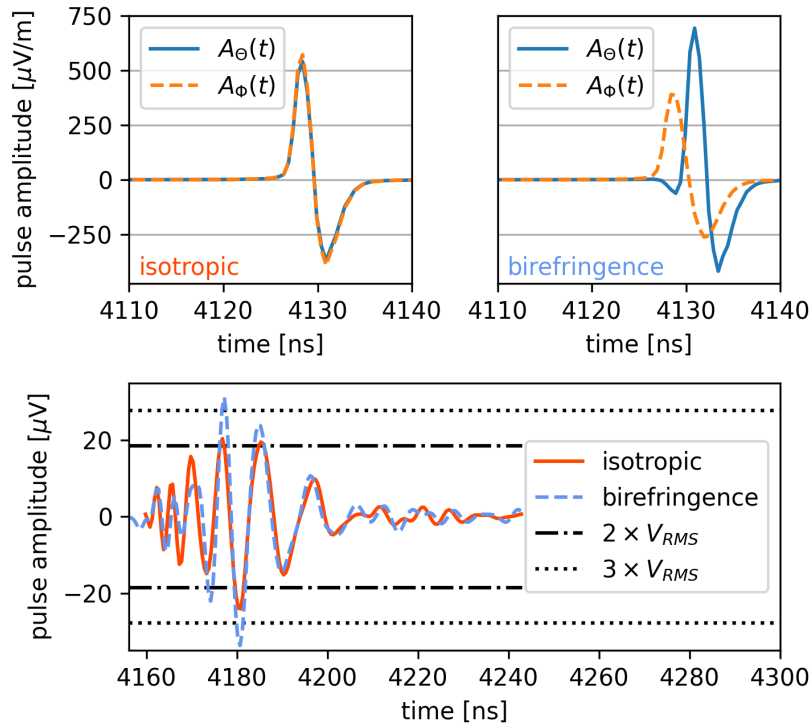


Figure 4: Example event that triggered the LPDA trigger in the birefringent medium but not in the isotropic medium. Top left: Electric field arriving at the LPDA antenna in the isotropic medium. Top right: Electric field arriving at the LPDA antenna in the birefringent medium. Bottom: Voltage trace arriving at the LPDA antenna in both media.

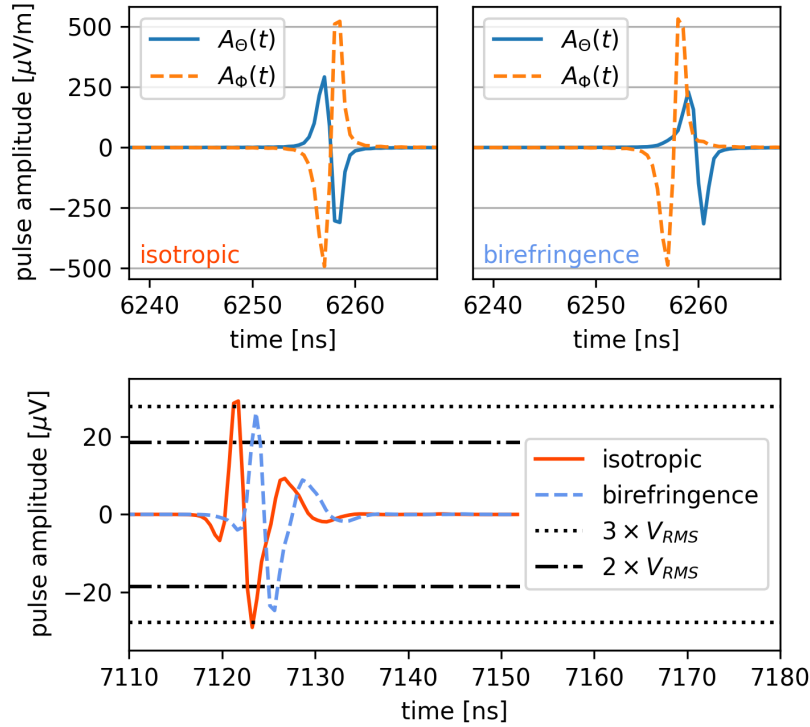


Figure 5: Example event that triggered the Vpol-trigger in the isotropic medium but not in the birefringent medium. Top left: Electric field arriving at the Vpol antenna in the isotropic medium. Top right: Electric field arriving at the Vpol antenna in the birefringent medium. Bottom: Voltage trace arriving at the Vpol antenna in both media.

on the polarization of the initially induced electric field by the neutrino interaction. Because the Vpol antennas are only sensitive to the (vertical projection) of the Θ polarization component, it is more likely that the antenna measures a reduced amplitude due to birefringence as some of the fluence is shifted into the polarization the Vpol antenna can't see. The LPDAs in turn are sensitive to (the horizontal projection) of both polarization components and thus are more likely to profit from birefringence. Figure 3 also shows that the deviation first increases with energy until approx. 10^{18} eV after which it decreases again. The rise with energy can be understood by the fact that propagation distances increase with energy and therefore the effect of birefringence. But at very high energies this is compensated by the amplitudes being so high that the pulses trigger either way.

Figure 4 shows an example of the electric fields and voltage traces of an event that triggered a $3 \times V_{RMS}$ -trigger of the LPDA antennas in a birefringent medium but did not trigger the same antenna in an isotropic medium. Figure 5 shows an example of the electric fields and voltage traces of an event that triggered the $3 \times V_{RMS}$ -trigger of the Vpol antenna in an isotropic medium but did not trigger the same antenna in a birefringent medium. Both examples show that even though the changes in amplitude/power of a pulse can be small, the trigger condition can be affected nonetheless.

The examples also show that the polarisation and arrival time can be affected significantly by

birefringence, however, the statistics in this study were too small to properly quantify and parametrize the effect as many events were simulated with birefringence that did not end up triggering either antenna. A larger study is planned with an order of magnitude more events where the pre-trigger simulation is more suited to trigger most events simulated in a birefringent medium. Furthermore, this study would allow for enough statistics to train a neural network on data in a birefringent medium to see how this systematic uncertainty truly affects event reconstruction.

5. Conclusion

In this contribution, we present a parametrization of the birefringence effect for in-ice radio propagation. The developed code can transform an electric field induced at any position into an electric field that is expected at any antenna position. The code is integrated into NuRadioMC and publically available. Measurements of the birefringence-induced time delays were compared to simulations and agreed within the uncertainties. The effective volume of a simplified radio station in an isotropic medium was compared to the same station in a birefringent medium. A trigger based on a deep Vpol antenna showed an up to 5% lower effective volume when including birefringence in the simulation while a trigger based on two perpendicular-oriented shallow LPDA antennas showed an up to 15% higher effective volume when including birefringence. Further studies with larger statistics are planned to investigate the effect of birefringence on polarization and time delays and the corresponding effect on event reconstruction.

References

- [1] **IceCube** Collaboration, M. G. Aartsen *et al.* *Science* **342** (2013) 1242856.
- [2] S. Barwick and C. Glaser. Arxiv: [2208.04971], (2023).
- [3] **RNO-G** Collaboration, J. A. Aguilar *et al.* *JINST* **16** (2021) P03025.
- [4] **IceCube-Gen2** Collaboration, M. G. Aartsen *et al.* *J. Phys. G* **48** (2021) 060501.
- [5] **IceCube-Gen2** Collaboration, R. Abbasi *et al.* *PoS ICRC2021* 1183.
- [6] **IceCube-Gen2** Collaboration. <https://icecube-gen2.wisc.edu/science/publications/TDR>.
- [7] T. M. Jordan *et al.* *Annals of Glaciology* **61** no. 81, (2020) 84–91.
- [8] A. Connolly *Phys. Rev. D* **105** (2022) 123012.
- [9] **IceCube** Collaboration, R. Abbasi *et al.* *The Cryosphere Discussions* (2022) 1–48.
- [10] N. Heyer and C. Glaser *Eur. Phys. J. C* **83** (2023) 124.
- [11] D. E. Voigt *U.S. Antarctic Program (USAP) Data Center* (2017) .
- [12] S. Barwick *et al.* *Journal of Glaciology* **51** no. 173, (2005) 231–238.
- [13] C. Glaser *et al.* *The European Physical Journal C* **80** (2020) 77.
- [14] J. A. Johnson *et al.* *Annals of Glaciology* **62** no. 84, (2021) 75–88.
- [15] **ARA** Collaboration, P. Allison *et al.* *Astroparticle Physics* **35** no. 7, (2012) 457–477.
- [16] S. W. Barwick *et al.* *IEEE Transactions on Nuclear Science* **62** no. 5, (2015) 2202–2215.
- [17] **ARIANNA** Collaboration, A. Anker *et al.* *JINST* **15** (2020) P09039.
- [18] A. F. Oskooi *et al.* *Computer Physics Communications* **181** no. 3, (2010) 687–702.